

Spin fluctuations in a random one-dimensional Heisenberg antiferromagnet: (CD₃)₄NMn_cCu_{1-c}Cl₃

Y. Endoh* and G. Shirane

Brookhaven National Laboratory, Upton, New York 11973

R. J. Birgeneau

Department of Physics and Center for Materials Science and Engineering, Massachusetts Institute of Technology, Cambridge, Massachusetts, 02139

Y. Ajiro

Department of Chemistry, Kyoto University, Kyoto, 606, Japan

(Received 31 August 1978)

In this paper we report a detailed neutron scattering study of the spin fluctuations in the random one-dimensional Heisenberg antiferromagnet (CD₃)₄NMn_cCu_{1-c}Cl₃ with $c = 0.93$ and $c = 0.85$. In this material the Mn-Cu exchange is only about 4% of the Mn-Mn exchange so that this system corresponds to a "weak-link" impure chain. For temperatures such that $k_B T > J_{\text{Mn-Cu}}$ percolationlike behavior is observed, while for $k_B T < J_{\text{Mn-Cu}}$ "weak-link" behavior obtains. The instantaneous magnetic correlations are found to be in good quantitative accord with the exact results for the random classical Heisenberg model. We also discuss briefly the spin-wave excitations at large q 's and the spin dynamics for $q \sim \kappa$, the inverse correlation length.

I. INTRODUCTION

In the past decade a rather large number of experimental and theoretical studies have been reported of the static and dynamic properties of one-dimensional (1D) magnets.¹ This work has been motivated both by the availability of exact theoretical results for 1D spin systems and by the realization that there are in nature real physical materials which correspond remarkably closely to ideal model Hamiltonian systems. The most extensively investigated material is (CD₃)₄NMnCl₃, tetramethylammonium-manganese-chloride (TMMC), which is a good physical approximation to the 1D classical Heisenberg antiferromagnet.² Parallel to these 1D studies, there have also been many experiments on disordered spin systems, especially magnetic insulating binary mixtures in which the "impurity" is either magnetic or nonmagnetic.³ Considerable progress has been made in both of these areas of research.

In this paper we report a neutron scattering study of the spin fluctuations in (CD₃)₄NMn_cCu_{1-c}Cl₃, that is, TMMC doped with Cu²⁺. It has been realized for some time that impurities may have particularly important effects in one dimension. For example, a single nonmagnetic impurity will break an infinite chain into two segments thus preventing the achievement of long-range order (LRO) even at $T = 0$ K. This then is the most elementary example of the percolation problem.⁴ In the language of marginal dimensionalities, for the percolation problem, the

lower marginal dimensionality $d^0 = 1$ and correspondingly the percolation concentration $c_p = 1$; we recall also that for a Heisenberg magnet $d^0 = 2$. Thus in a one-dimensional spin system the percolation multicritical point occurs at $c_p = 1$, $T = 0$ K. For $c < 1$ or $T > 0$ K, the system cannot exhibit LRO. For *classical spins* exact solutions^{5,6} are available for the spin correlations for 1D dilute Heisenberg magnets as a function of both c and T .

In the system TMMC:Cu the Cu²⁺ ($S = \frac{1}{2}$) ions are, of course, magnetic. However the Mn-Cu interaction energy is very much less than the Mn-Mn exchange.^{7,8} This system then rests in a very interesting intermediate regime. Indeed it is a close analog to the often used model of 1D conducting chains with intermittent weak links. Intuitively we might expect that at temperatures high compared with the Mn-Cu exchange coupling the Cu²⁺ ions would be effectively noninteracting and TMMC:Cu would then exhibit percolation behavior. However, as the temperature is lowered we would expect a crossover into a region where correlations between the Mn segments would be communicated through the Cu²⁺ spins. The nature of this crossover and the behavior in these "percolation" and "weak-link" regimes are clearly of considerable interest. Furthermore, exact solutions have been obtained for the spin correlations for this problem as well, in the limit that the Mn²⁺ and Cu²⁺ spins are treated as classical variables.^{5,6} This classical spin model is known to describe pure TMMC very well²; it will be most interesting to see if similar accord is obtained for TMMC:Cu.

The format of this paper is as follows. In Sec. II we review the exact classical spin results as they apply to TMMC:Cu. In Sec. III we describe the experimental techniques and results. Section IV gives the analysis, comparison with theory, and conclusions.

We should note that after completion of this work we received a preprint reporting similar measurements on TMMC:Cu by Boucher *et al.*⁹ Their study of the static correlations was much less extensive than ours and further it was carried out from a somewhat different vantage point. Hence we give a full report of our own experiments. We have, however, obtained comparable results for the dynamics; since the Boucher *et al.*⁹ work is already published we give only a very brief summary of our spin-wave measurements.

II. THEORY

As we noted above, exact results have been obtained for the instantaneous correlations for the impure classical Heisenberg chain; the theory involves a simple generalization of the methods used for the pure systems¹⁰ with, of course, an appropriate averaging over the random variables. Results relevant to TMMC:Cu have been reported both by Tonegawa *et al.*⁵ and by Thorpe.⁶ In this paper we shall follow the discussion of Thorpe. The Hamiltonian is written

$$\mathcal{H} = - \sum_{\alpha\beta} J_{\alpha\beta} \vec{S}_{\alpha}^i \cdot \vec{S}_{\beta}^{i+1}, \quad (1)$$

where α, β stand for Mn with probability c , and

Cu with probability $1 - c$. We note also that the Z component of the magnetization is given by

$$M_{\alpha}^z = g_{\alpha} \mu_B S_{\alpha}^z. \quad (2)$$

For Mn^{2+} $S = \frac{5}{2}$ while for Cu^{2+} $S = \frac{1}{2}$. Unfortunately Eq. (1) is not exactly soluble for real quantum-mechanical spins. We therefore consider instead the classical Hamiltonian

$$\mathcal{H} = - \sum_i J_{\alpha\beta} \vec{\sigma}_{\alpha}^i \cdot \vec{\sigma}_{\beta}^{i+1} \quad (3)$$

with

$$J_{\alpha\beta} = J_{\alpha\beta} [S_{\alpha}(S_{\alpha} + 1)S_{\beta}(S_{\beta} + 1)]^{1/2}.$$

Here the $\vec{\sigma}_{\alpha}^i$ are classical unit vectors. For the magnetization we make the correspondence

$$\begin{aligned} M_{\alpha}^z &= g_{\alpha} \mu_B S_{\alpha}^z \\ &= g_{\alpha} \mu_B |S_{\alpha}| \sigma_{\alpha}^z \\ &= G_{\alpha} \sigma_{\alpha}^z. \end{aligned} \quad (4)$$

Thus for Mn^{2+} , $G_{\alpha} = 5\mu_B$ while for Cu^{2+} , $G_{\alpha} \approx 1\mu_B$. We remind the reader that in a neutron scattering experiment in the dipole approximation it is the magnetization-magnetization correlation function rather than the spin-spin correlation function which is measured.

We quote here explicitly Thorpe's final result for the magnetization-magnetization correlation function

$$\begin{aligned} \mathcal{S}(q) &= (1/N) \langle \vec{M}_{\alpha}(q) \cdot \vec{M}_{\beta}(q) \rangle \\ &= c \mathcal{S}^{\text{Mn}}(q) + (1-c) \mathcal{S}^{\text{Cu}}(q), \end{aligned} \quad (5)$$

where

$$\mathcal{S}^{\text{Mn}}(q) = 2\text{Re} \left(\frac{G_{\text{Mn}}^2 + e^{iqa}(1-c)(G_{\text{Mn}}G_{\text{Cu}}U_{\text{Mn-Cu}} - G_{\text{Mn}}^2U_{\text{Cu-Cu}})}{1 - e^{iqa}cU_{\text{Mn-Mn}} - e^{iqa}(1-c)U_{\text{Cu-Cu}} + 2e^{iqa}c(1-c)(U_{\text{Mn-Mn}}U_{\text{Cu-Cu}} - U_{\text{Mn-Cu}}^2)} \right) - 1 \quad (6)$$

and a similar definition holds for $\mathcal{S}^{\text{Cu}}(q)$. Here

$$U_{\alpha-\beta} = \coth(J_{\alpha\beta}/kT) - kT/J_{\alpha\beta}. \quad (7)$$

The constant a is the separation between nearest-neighbor spins along the chain. It may be easily verified that the above reduces to the pure chain result by setting $c = 1$. In analyzing our experi-

mental results we shall use the full expression Eq. (6). However, in order to discuss the physics underlying Eq. (6) it is appropriate to consider two regimes.

(i) *Percolation regime*: $J_{\text{Cu}} - J_{\text{Cu}}$, $J_{\text{Mn-Cu}} \ll kT \ll J_{\text{Mn-Mn}}$. In this regime the results go over directly to those of the dilute magnetic chain. Explicitly, in the above temperature range, for

antiferromagnetic coupling

$$\begin{aligned} U_{\text{Mn-Mn}} &\rightarrow -1 - kT/J_{\text{Mn-Mn}}, \\ U_{\text{Mn-Cu}}, U_{\text{Cu-Cu}} &\rightarrow 0. \end{aligned} \quad (8)$$

It may be easily verified that in this limit for a Heisenberg antiferromagnet

$$\hat{s}(q) \simeq \frac{A}{(\kappa a)^2 + [qa - (2n+1)\pi]^2}, \quad (9)$$

where

$$\kappa a = \frac{1-c}{\sqrt{c}} + \frac{kT}{|J_{\text{Mn-Mn}}|} \frac{1+c}{2\sqrt{c}} \quad (10a)$$

and

$$A = G_{\text{Mn}}^2 \left(\frac{1-c^2}{c} + \frac{kT}{|J_{\text{Mn-Mn}}|} \frac{1+c^2}{c} \right) \quad (10b)$$

which are, of course, the results for the dilute 1D classical Heisenberg antiferromagnet. Here $\kappa = 1/\xi$ is the inverse correlation length. The physical interpretation of the above results is clear. Following Ref. 4, Eq. (10a) for κ may be written $\kappa = \kappa_G + \kappa_T$ where κ_G and κ_T are the inverse correlation lengths resulting from geometrical and thermal disorder, respectively. κ_G and κ_T go to zero linearly with $1-c$ and T , respectively. As noted previously by several authors,¹¹ in percolation multicritical language this corresponds to correlation length exponents $\nu_p = \nu_t = 1$ so that the crossover exponent is also 1.

(ii) *Weak-Link Regime:* $kT < J_{\text{Cu-Cu}}, J_{\text{Mn-Cu}}, J_{\text{Mn-Mn}}$. In this regime for antiferromagnetic coupling

$$U_{\alpha\beta} \rightarrow -1 + kT/|J_{\alpha\beta}|.$$

Once again obtains a Lorentzian profile, Eq. (9), but with

$$\kappa a = kT \left(\frac{c^2}{|J_{\text{Mn-Mn}}|} + \frac{2c(1-c)}{|J_{\text{Mn-Cu}}|} + \frac{(1-c)^2}{|J_{\text{Cu-Cu}}|} \right) \quad (11a)$$

and

$$A = 2\kappa [cG_{\text{Mn}} + (1-c)G_{\text{Cu}}]^2. \quad (11b)$$

The above assumes that all interactions are antiferromagnetic. There is in addition a small correction term to Eq. (9) which, in the limit $\kappa \rightarrow 0$, corresponds to normal incoherent scattering. In the region

$$\frac{2(1-c)J_{\text{Mn-Mn}}}{c J_{\text{Mn-Cu}}} \gg 1, \quad (1-c) \ll 1$$

the above corresponds simply to a renormalized 1D chain problem with well-aligned Mn^{2+} segments acting effectively as single spins with inverse length $1-c$ becoming correlated through the intervening Cu^{2+} ions.

It is clear from the above the intuitive arguments

which we presented in the Introduction are indeed confirmed by the exact results for classical chains. Let us now consider various additional details involved in applying the above theory to $(\text{CD}_3)_4\text{NMn}_c\text{Cu}_{1-c}\text{Cl}_3$. Firstly the exchange interaction should indeed be of the Heisenberg form. For pure TMMC, $J_{\text{Mn-Mn}} = -13.0 \pm 0.3$ K. In addition, there is the magnetic dipole-dipole interactions between the magnetic ions; this term introduces an XY anisotropy which in turn enhances the xx and yy spin correlations relative to the zz correlations.¹² Both the original TMMC quasielastic neutron scattering experiments² and the measurements to be reported in this paper were carried out in such a way that one effectively measures $\hat{s}^{xx}(q) + \hat{s}^{yy}(q)$, that is, one measures the transverse correlations. It was found empirically in the pure TMMC experiments that the classical Heisenberg theory works very well for the transverse correlations provided that one uses a renormalized exchange $J_{\text{Mn-Mn}} = -15.4$ K. This corresponds to $J_{\text{Mn-Mn}} = 135$ K. The inelastic experiments to be discussed in Sec. III verify that the $J_{\text{Mn-Mn}}$ is unchanged in the doped samples; hence we shall take the above value as a fixed quantity in the theoretical analysis. Previous experiments by Dupas and Renard⁷ and by Richards⁸ suggest $J_{\text{Mn-Cu}} \approx 3$ K corresponding to $|J_{\text{Mn-Cu}}/J_{\text{Mn-Mn}}| \approx 0.06$. We should note that this value also incorporates to first order any effects of next-nearest-neighbor Mn-Mn interactions. As we shall see in Sec. IV our experiments suggest a value for $|J_{\text{Mn-Cu}}/J_{\text{Mn-Mn}}|$ close to, but slightly smaller than, the above value. Such differences may, of course, simply reflect errors in the classical spin approximation. Finally, no information is available for the Cu-Cu exchange either from our work or from previous experiments.

III. EXPERIMENTS

A. Sample preparation and characterization

The single crystals used in the present neutron scattering studies were prepared in a manner quite similar to that described by Hutchings *et al.*² The principal difference here is the starting solutions. In order to grow single crystals which contain randomly distributed magnetic ions, and in order at the same time to control the chemical concentration of metallic ions, we prepared a mixture of $\text{MnCl}_2 \cdot 4\text{D}_2\text{O}$ and $\text{CuCl}_2 \cdot 2\text{D}_2\text{O}$. This mixture was added to a solution of deuterated tetramethyl ammonium chloride in 10-vol. % DCl. The dissolved solution was placed in a dessicator over CaSO_4 . Seed crystals in the form of thin needles were extracted from the

solution at an early stage. A seed crystal was then situated in the same solution at a fixed temperature of 40 °C in order to grow a large crystal. Using this technique we have obtained several crystals of $\approx 0.5 \text{ cm}^3$ in volume.

The addition of Cu makes a noticeable change of color to dark brown but does not make any change of crystal habit. Although considerable care was taken in the growth, we found that a given crystal may contain a Cu^{2+} concentration quite different from the starting solution. This discrepancy was very small for some samples and was surprisingly large for others. In all studies of mixed crystals, especially those in which the results are a sensitive function of the concentrations of one of the constituents, some difficulties are encountered in determining precisely the concentrations of the explicit samples studied. In this case we have used a compromise technique. Firstly, chemical analysis of the constituents was obtained for small slices cleaved from the tail sections of the crystals. Simultaneously, using neutron diffraction techniques, we have determined accurately the c -axis lattice constants of each of the crystals; this then gives the lattice constant averaged over any possible Cu concentration gradient across the sample. We show in Fig. 1, the obtained reciprocal-lattice constant for the samples as a whole versus the Cu^{2+} concentration as determined from the chemical analysis of the tail section. The experi-

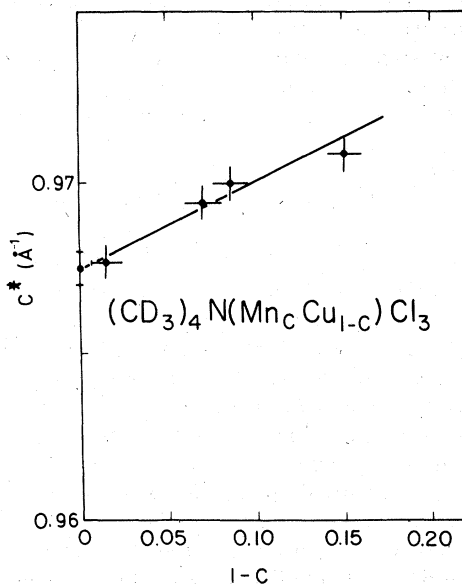


FIG. 1. Reciprocal-lattice constant $c^* = 2\pi/c$ of $(\text{CD}_3)_4\text{NMn}_c\text{Cu}_{1-c}\text{Cl}_3$ at 293 K. The concentration c is determined by chemical analysis.

mental points fall on a smooth, nearly linear, curve to an accuracy of about 1% in the Cu concentration. This internal consistency leads us to believe that we know the actual Cu concentration to an accuracy of 1%. As we shall see later, our neutron scattering results imply Cu concentrations close to those deduced from the lattice-constant curve, Fig. 1. To be totally candid, however, we should emphasize that if a large discrepancy occurred we would undoubtedly question the above technique.

Both the symmetry of the crystal structure and the 128-K crystallographic phase transition² were found to be independent of Cu concentration up to at least 20% Cu. In addition, the transverse-lattice parameters also changed very little with substitution of the Cu for Mn. Two crystals with 7% and 15% Cu concentration were chosen for detailed studies of the spin fluctuations at low temperatures. Both were approximately 0.5 cm^3 in volume. They were oriented such that the $(h0l)$ zone was in the scattering plane. Each crystal was mounted in a standard aluminum sample can which was in turn attached to the tail section of the cryostat. Temperatures down to 1.01 K could be obtained.

B. Quasielastic scattering experiments

The experiments were performed on a double-axis spectrometer at the Brookhaven high flux beam reactor using neutrons of wavelength 2.443 Å. The neutrons were monochromatized using a vertically bent pyrolytic graphite monochromator together with an oriented graphite filter to eliminate higher-order neutrons. Most of the scans were carried out using 10-min collimation before and after the sample. This yields a net longitudinal in-plane resolution of about 0.01 Å^{-1} full width at half maximum. As is well known, the magnetic scattering in one-dimensional magnets occurs in *plane*² perpendicular to the chain axis direction \vec{c} . As originally demonstrated by Birgeneau *et al.*,¹³ the integration over the energy may be carried out essentially exactly at fixed q_c by choosing the scattering geometry such that the outgoing neutron direction is perpendicular to \vec{c} . In this configuration, the energy integration involves exclusively changes in \vec{q}_\perp for the neutron; in a true 1D system the scattering will be independent of the momentum component perpendicular to the chain axis. All experiments were carried out in this configuration.

The experimental results are qualitatively similar to those obtained in pure TMMC.² Pronounced 1D scattering is observed at $(h0l)$ independent of h and centered about $l = 0, 1, 2, \dots$ [We

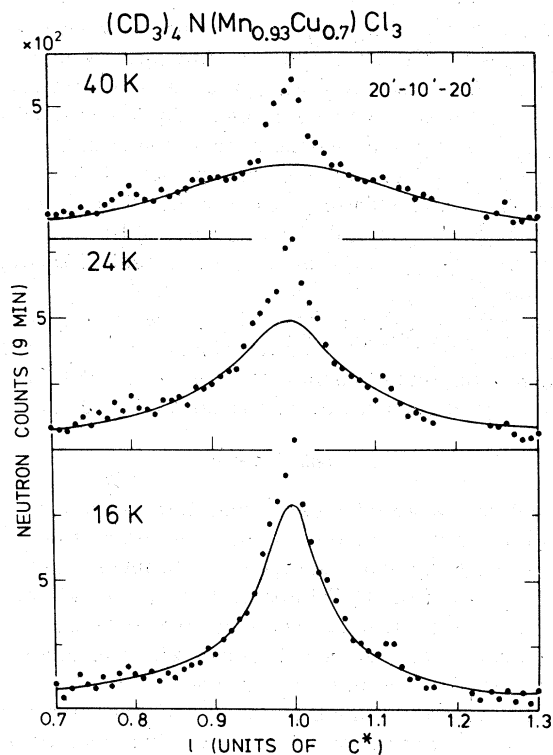


FIG. 2. Quasielastic scans across the planes in the $c = 0.93$ sample. The scans were made in the $(h0l)$ plane with h fixed at 0.3 reciprocal lattice units. The solid lines are the results of fits of Lorentzians to the wings as described in the text. Note that the nuclear scattering near $l=1$ is clearly separable at 24 and 40 K. For these scans the collimation was 10 min before and 20 min after the sample.

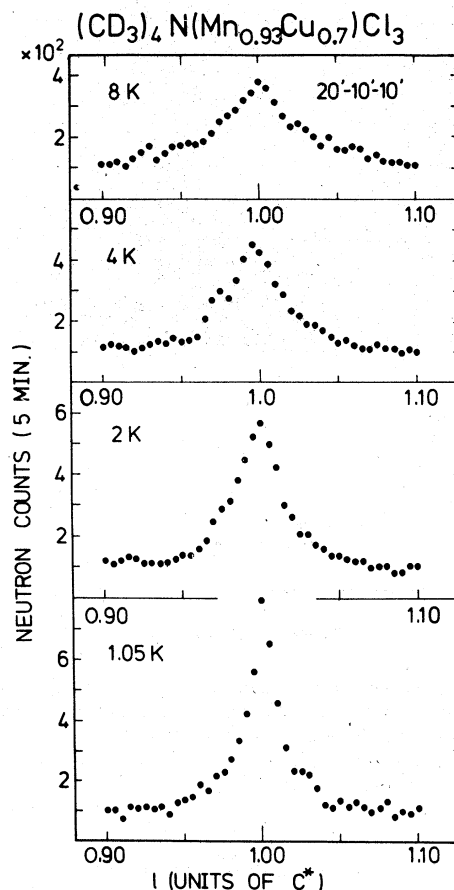


FIG. 3. Quasielastic scans across the plane in the $c = 0.93$ sample at low temperatures. The scan geometry and configuration were as in Fig. 2 but with 10-min collimation after the sample.

note that in TMMC the hexagonal lattice c is equal to $2a$ where a is the nearest-neighbor separation along the MnCl_3 chains. Hence the magnetic scattering should occur at $q = (2n+1)\pi/a = (2n+1)2\pi/2a = (2n+1)c^*$.

As observed previously,² the 1D scattering has very different characteristics for l even and for l odd. For even l , the scattering is purely nuclear in origin whereas the scattering around $l=1, 3, \dots$ contains contributions from both nuclear and magnetic scattering. We show in Figs. 2 and 3 a series of scans across the $l=1$ magnetic plane in the 7-at.% Cu sample at $(0.3, 0, l)$. At 40 and 24 K the two components to the scattering are clearly separable. The solid lines in Fig. 2 represents fits of the wings to a Lorentzian [Eq. (8)] convoluted with the instrumental resolution function. The residual nuclear central component is resolution limited.

At lower temperatures such a simple separation was no longer possible. In order to determine the magnetic part of the scattering at lower temperatures we used the technique employed in the pure TMMC studies.² Briefly, the nuclear scattering at $(0.3, 0, 1)$ was assumed to be identical to that at $(0.3, 0, 2)$ to within a constant scale factor. This scale factor could be readily determined from the high-temperature ($T > 20$ K) scans. Scans identical to those shown in Figs. 2 and 3 were then carried out simultaneously across the $l=2$ plane. This scattering, appropriately scaled, was then subtracted from the $l=1$ scattering at each temperature.

Least-squares fits were carried out of a Lorentzian convoluted with the resolution function of the spectrometer to the residual 1D magnetic scattering. In general, these fits were quite satisfactory, with goodness-of-fit parameter

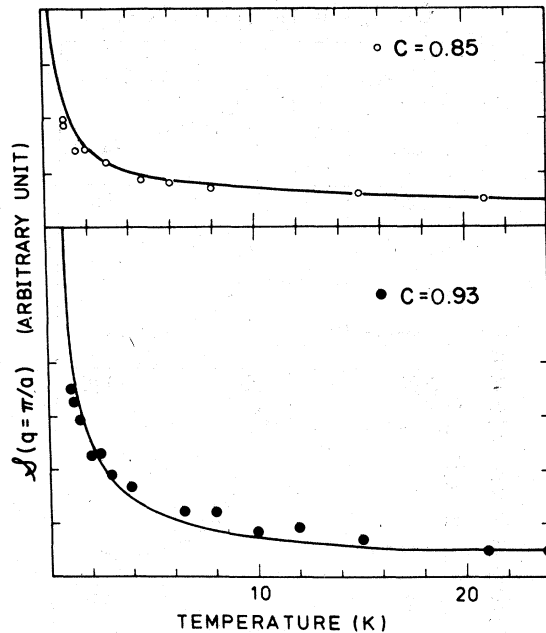


FIG. 4. Deconvoluted quasielastic peak intensity vs temperature in the $c=0.93$ and $c=0.85$ samples. The solid lines are the results of the classical theory as described in the text. The scale factor was fixed by the high-temperature points.

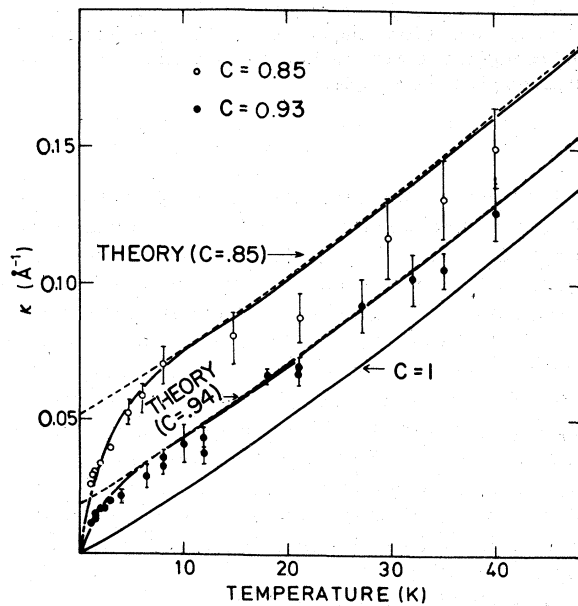
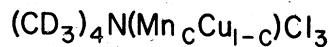


FIG. 5. Inverse correlation length vs temperature. The solid line corresponds to the full theory, Eq. (6), with the parameters given in the text. The dashed line corresponds to the percolation limit with $J_{\text{Mn-Cu}} = 0$.

χ^2 between 1 and 2 at all temperatures. We show in Fig. 4 the deconvoluted peak intensity, which is just $\delta(q = \pi/a)$, as a function of temperature for the $c=0.93$ and $c=0.85$ samples. The corresponding results for the inverse correlation length κ are shown in Fig. 5. It is evident that κ indeed has the behavior anticipated from our discussion in Sec. II. We shall discuss these results quantitatively in the context of the classical theory in Sec. IV.

Boucher *et al.*⁹ have investigated two concentrations $c=0.97$ and 0.92 for temperatures up to 15 K. When data points overlap, the results on $c=0.92$ are in good accord with our results on $c=0.93$.

C. Spin dynamics

Inelastic scattering experiments were carried out both to determine the spin-wave dispersion relation in the doped samples and to investigate the effects of the Cu^{2+} impurities on the long-wavelength spin dynamics. The measurements were performed using standard triple-axis techniques. Scans were made in the constant- Q mode of operation with either the incoming or outgoing neutron energy fixed at 13.7 meV. The spin-wave measurements were performed at 1.1 K in both the $c=0.93$ and $c=0.85$ samples. Well-defined peaks arising from purely 1D spin-wave excitation were observed for q 's varying from $qa = \frac{1}{2}\pi$ down

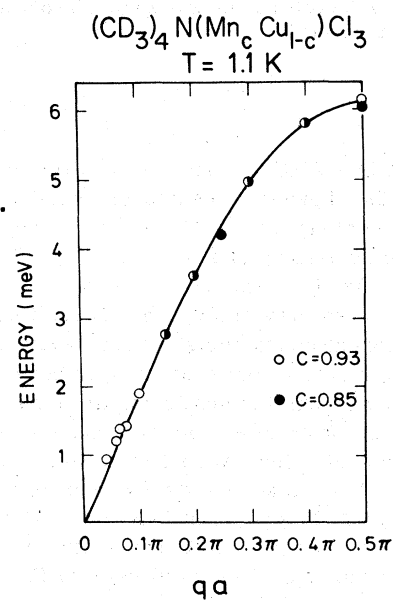


FIG. 6. Spin-wave dispersion relation for the Mn^{2+} magnetic excitations in the $c=0.93$ and $c=0.85$ samples at 1 K. The solid line represents the magnon dispersion curve for pure TMMC.

to $|qa - \pi| \gtrsim 2\kappa$. The consequent dispersion relations for the two samples are shown in Fig. 6. The solid line is the measured dispersion relation in pure TMMC. It is evident that the Cu impurities have remarkably little effect on the Mn^{2+} excitation peak energies. Correspondingly, in our discussion of the quasielastic measurements on the doped samples we may validly use $J_{\text{Mn-Mn}}$ as determined for the pure system; hence this will not be an adjustable parameter in any comparisons between experiment and theory.

We have also briefly surveyed the dynamics in the region $q \approx \kappa$. As we noted previously, this has been discussed extensively by Boucher *et al.*⁹ in their TMMC:Cu experiments. Our experimental results are supportive of theirs, that is, we also find that underdamped spin-wave excitations are only observed for $q \gtrsim 2\kappa$. This is in accord with our expectations based both on physical grounds and on the high-resolution experiments of Shirane and Birgeneau¹⁴ in TMMC.

IV. DISCUSSION AND CONCLUSIONS

As we noted in the previous section the quasielastic results correspond closely to our qualitative expectations. We now wish to make a quantitative comparison between the experimental results shown in Figs. 4 and 5 and the classical theory. The staggered structure factor may be simply calculated from Eq. (5) with $q = \pi/a$ and with, of course, an appropriate set of interaction parameters. In order to obtain the inverse correlation length κ from Eq. (5) we have calculated the full theoretical cross section $\mathcal{S}(q)$ and then deduced from it the actual half width at half maximum. The parameters required to calculate $\mathcal{S}(q)$ are $J_{\text{Mn-Mn}}$, $J_{\text{Mn-Cu}}$, $J_{\text{Cu-Cu}}$, $G_{\text{Mn}}/G_{\text{Cu}}$, and c . For reasonable ranges of parameter values the computed results are insensitive to two of the parameters, $J_{\text{Cu-Cu}}$ and the ratio $G_{\text{Mn}}/G_{\text{Cu}}$. Explicitly, Cu-Cu pairs only effect the results for very long correlation lengths, that is, $\kappa a \lesssim 2(1-c)^2$, a region not probed in these experiments in either sample. Accordingly, we have taken $J_{\text{Cu-Cu}} = 0$ in the actual calculations; we have also verified that the results are little changed if, for example, we take $J_{\text{Cu-Cu}} = J_{\text{Cu-Mn}}$. For the relative Mn^{2+} and Cu^{2+} moments we have taken $G_{\text{Mn}}/G_{\text{Cu}} = 5$, that is, the ratio of the spin quantum numbers. This large ratio means simply that the scattering is completely dominated by the Mn^{2+} spins, concomitantly a small error in the relative Cu^{2+} scattering strength has no discernible effect on the results. The spin-wave measurements (Fig. 6) suggest that we should take $J_{\text{Mn-Mn}}$ to be identical in all samples. We remind the reader that in order to obtain quantitative accord between experiment

and the classical Heisenberg theory for pure TMMC it was necessary to use an enhanced value for $J_{\text{Mn-Mn}}$. We have suggested that this may reflect the influence of the dipolar XY anisotropy which is not included in the theory. We shall assume that this enhancement effect is identical in the doped samples and accordingly we take $J_{\text{Mn-Mn}} = 135$ K.

We consider firstly the "percolation" region, $T > 10$ K. From Eq. (10a) we anticipate that κa extrapolated to $T = 0$ should just be equal to $1 - c/\sqrt{c}$. This gives $c = 0.94 \pm 0.01$ and $c = 0.85 \pm 0.01$ in excellent accord with the values of 0.93 ± 0.01 and 0.85 ± 0.01 suggested by the lattice constants and chemical analysis (see Sec. II A). We show as the dashed lines in Fig. 5 the classical theory results for κ [cf. Eq. (10a)] with $c = 0.94$ and $c = 0.85$ and with $J_{\text{Mn-Cu}} = 0$. The role of the Mn-Cu coupling below 10 K is apparent. We now consider the effect of the Mn-Cu coupling. The full lines correspond to the classical theory with $|J_{\text{Mn-Cu}}| = 5.4$ K. The agreement, especially at low temperatures, is very good. An interesting feature is that the results are nearly independent of the sign of $J_{\text{Mn-Cu}}$. This occurs simply because the order between successive Mn^{2+} segments is identical whether the intervening Cu^{2+} spin is parallel or antiparallel to its neighboring Mn^{2+} spins; further the scattering power of the Cu^{2+} ion is sufficiently weak that it has little effect on $\mathcal{S}(\pi/a)$. We show in Fig. 4 the results of the classical theory for $\mathcal{S}(\pi/a)$ with the parameters as above. The overall scattering intensity is normalized at high temperatures. Again, the agreement between the classical theory and experiment is excellent.

We find, therefore, that the classical theory works nearly as well for the random chain as it does for the pure system. There is a slight discrepancy for κ in the $c = 0.85$ sample at high temperatures; however, this may simply reflect an error in the effective renormalization of $J_{\text{Mn-Mn}}$ due to the dipolar anisotropy. The "percolation" and "weak-link" regimes are clearly observed. Further, the predicted percolation behavior, $\kappa = \kappa_T + \kappa_G$, is obtained. More experiments and theory in higher dimensions would be most valuable in order to determine if this is a general result for magnets near the percolation threshold. Finally our value for $|J_{\text{Mn-Cu}}|/J_{\text{Mn-Mn}} = 0.04 \pm 0.01$ is in good agreement with the result $J_{\text{Mn-Cu}}/J_{\text{Mn-Mn}} = -0.06 \pm 0.01$ deduced from resonance and susceptibility measurements.^{7,8} Clearly experiments down to 0.1 K would be most valuable in order to elucidate the role of Cu-Cu impurity pairs. Similarly, studies of the long-wavelength spin dynamics would be most interesting in this temperature regime.

ACKNOWLEDGMENTS

We wish to acknowledge many helpful discussions with M. Blume, Y. Imry, H. J. Mikeska, and H. Shiba. Work at Tohoku University was supported by a Grant for Fundamental Research

in Chemistry, Japan Society for the Promotion of Science. Work at Brookhaven was supported by the Division of Basic Energy Sciences, Department of Energy, under Contract No. EY-76-C-02-0016. Research at M. I. T. was supported by the NSF under Contract No. DMR78-02397.

- *On leave from the Dept. of Physics, Tohoku University, Sendai, 980, Japan, and now returned.
- ¹M. Steiner, J. Villain, and C. G. Windsor, *Adv. Phys.* **25**, 87 (1976); R. J. Birgeneau and G. Shirane, *Phys. Today* **31** (12), 32 (1978).
- ²R. J. Birgeneau, R. Dingle, M. T. Hutchings, G. Shirane, and S. L. Holt, *Phys. Rev. Lett.* **26**, 718 (1971); M. T. Hutchings, G. Shirane, R. J. Birgeneau, and S. L. Holt, *Phys. Rev. B* **5**, 1999 (1972).
- ³For a review see R. A. Cowley, *A. I. P. Conf. Proc.* **29**, 243 (1976).
- ⁴R. J. Birgeneau, R. A. Cowley, G. Shirane, and H. J. Guggenheim, *Phys. Rev. Lett.* **37**, 940 (1976).
- ⁵T. Tonegawa, H. Shiba, and P. Pincus, *Phys. Rev. B* **11**, 4683 (1975); T. Tonegawa, *Phys. Rev. B* **14**, 3166 (1976).

- ⁶M. F. Thorpe, *J. Phys. (Paris)* **36**, 1177 (1975).
- ⁷C. Dupas and J. P. Renard, *Phys. Lett. A* **55**, 181 (1975); *Phys. Rev. B* **18**, 401 (1978).
- ⁸P. M. Richards, *Phys. Rev. B* **10**, 805 (1974).
- ⁹J. P. Boucher, C. Dupas, W. J. Fitzgerald, K. Knorr, and J. P. Renard, *J. Phys. (Paris)* **39**, L-86 (1978).
- ¹⁰M. E. Fisher, *Am. J. Phys.* **32**, 343 (1964).
- ¹¹M. J. Stephen and G. Grest, *Phys. Rev. Lett.* **38**, 567 (1977); P. J. Reynolds, H. E. Stanley, and W. Klein, *J. Phys. A* **10**, L203 (1977).
- ¹²D. Hone and A. Pires, *Phys. Rev. B* **15**, 323 (1977).
- ¹³R. J. Birgeneau, J. Skalyo Jr., and G. Shirane, *Phys. Rev. B* **3**, 1736 (1971).
- ¹⁴G. Shirane and R. J. Birgeneau, *Physica* **86-88B**, 639 (1977).